

## Discrete Breathers in Nonlinear Lattices: Experimental Detection in a Josephson Array

E. Trías,<sup>1</sup> J. J. Mazo,<sup>1,2</sup> and T. P. Orlando<sup>1</sup>

<sup>1</sup>*Department of Electrical Engineering and Computer Science, Massachusetts Institute of Technology, Cambridge, Massachusetts 02139*

<sup>2</sup>*Departamento de Física de la Materia Condensada and ICMA, CSIC-Universidad de Zaragoza, E-50009 Zaragoza, Spain*  
(Received 7 April 1999)

We present the experimental detection of discrete breathers in an underdamped Josephson-junction array. Breathers exist under a range of dc current biases and temperatures, and are detected by measuring dc voltages. We find that the maximum allowable bias current for the breather is proportional to the array depinning current, while the minimum current seems to be related to a junction retrapping mechanism. We have observed that this latter instability leads to the formation of multisite breather states in the array. We have also studied the domain of existence of the breather at different values of the array parameters by varying the temperature.

PACS numbers: 74.50.+r, 45.05.+x, 63.20.Pw, 85.25.Cp

Discrete breathers have been mathematically proven to be generic solutions for the dynamics of nonlinear coupled oscillators [1,2] and have been theoretically studied in depth in the last few years [3,4]. These solutions are characterized by an exponential localization of the energy. Their existence results from the nonlinearity and discreteness of the system. Discreteness is essential to preventing resonances between the breather and the system characteristic frequencies. Surprisingly, this localization occurs in perfectly regular systems, so that it is intrinsic and different from Anderson localization or any other localization due to the presence of imperfections or impurities in the lattice. Thus, discrete breathers are also known as intrinsic localized modes. They have been proposed to exist in diverse systems such as in spin wave modes of antiferromagnets [5], DNA denaturation [6], and the dynamics of Josephson-junction networks [7–9]. Also, they have been shown to be important in the dynamics of mechanical engineering systems [10,11].

In this Letter we present the experimental detection of discrete breathers in an underdamped Josephson-junction array. Anisotropic Josephson-junction ladders were proposed in [7] as a model system to experimentally study discrete breathers biased by ac external currents. In [8] we numerically found that a dc external current is sufficient to excite and support breathers in the array. However, unlike simulations in [8] and [9], the junctions in our experiment have a nonlinear resistance and a characteristic gap voltage.

Recent work on the experimental detection of discrete breathers in a low-dimensional crystal [12] and an antiferromagnet [13] have been published. Both experiments excited breathers with ac driving forces while our experiment uses dc driving currents and also allows us to excite and detect discrete breathers in a controlled way.

A Josephson junction consists of two superconducting leads separated by a thin insulating barrier. Because of the Josephson effect, it behaves as a solid-state nonlinear oscillator and is modeled by the same dynamical equa-

tions that govern the motion of a driven pendulum [14]:  $i = \ddot{\varphi} + \Gamma \dot{\varphi} + \sin\varphi$ . The response of the junction to a current is measured by the voltage of the junction which is given by  $v = (\Phi_0/2\pi)d\varphi/dt$ . By coupling junctions it is possible to construct solid-state physical realizations of nonlinear oscillator systems. Moreover, since the parameters, such as  $\Gamma$ , vary with temperature, a range of parameter space can be studied easily with each sample.

The inset of Fig. 1 shows a schematic of the anisotropic ladder array. The junctions are fabricated using a Nb-Al<sub>2</sub>O<sub>x</sub>-Nb trilayer technology with a critical current density of 1 kA/cm<sup>2</sup>. The current is injected and extracted through bias resistors in order to distribute the external current as uniformly as possible through the array. These resistors are large enough so as to minimize any deleterious effects on the dynamics. The anisotropy of the array  $h$  is the ratio of areas of the horizontal to vertical junctions. In our arrays  $h = 1/4$  and  $h = I_{ch}/I_{cv} = R_v/R_h = C_h/C_v$ , and  $\Gamma_v = \Gamma_h = \Gamma$  (see [8] for a derivation of a circuit model of the array). As shown in the schematic, we placed voltage probes at various junctions to measure the voltages of both horizontal and vertical junctions.

In Fig. 1 we show a typical current-voltage,  $I$ - $V$ , characteristic of the array. As the applied current increases from zero we measure the time-averaged voltage of the 9th junction. The junction starts at a zero-voltage state and remains there until it reaches the array's depinning current  $I_{dep}$  at about 2 mA. When the current is larger the junction switches from zero-voltage state to the junction's superconducting gap voltage,  $V_g$ , which at this temperature is 2.5 mV. At this point all of the vertical junctions are said to be rotating and the array is in its whirling state. One of the effects of this gap voltage is to substantially affect the junction's resistance, and thereby damping, in a complicated nonlinear way. The current can be further increased until the junction reaches its normal state and it behaves as a resistor,  $R_n$ , of 5  $\Omega$ . As the current decreases the junction returns to the gap voltage and then to its zero-voltage

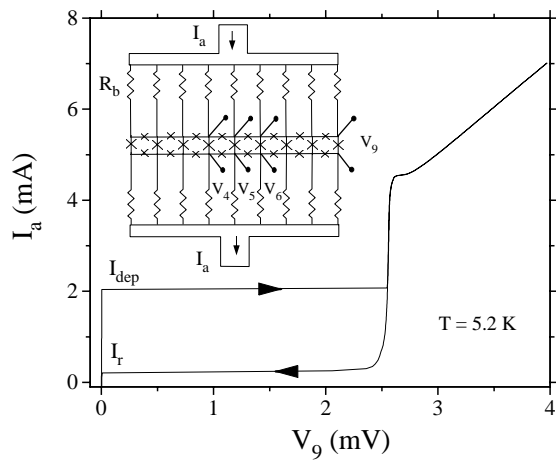


FIG. 1. Current-voltage characteristic of an anisotropic Josephson junction array when no breathers are excited. The hysteresis between the depinning current ( $I_{dep} \approx 2$  mA) and the retrapping current ( $I_r \approx 0.2$  mA) is shown. Inset: Schematic of the anisotropic ladder array. Vertical junctions have four times the area of the horizontal ones. Current is injected through bias resistors  $R_b$ . There are voltage probes in the fourth, fifth, sixth, and ninth vertical junctions to measure  $V_4$ ,  $V_5$ ,  $V_6$ , and  $V_9$ . The voltage probes can also be used to measure the top horizontal junctions in the middle which we denote as  $V_{4T}$  and  $V_{5T}$ .

state at the retrapping current,  $I_r$ , of  $\approx 0.2$  mA. The hysteresis loop between  $I_{dep}$  and  $I_r$  is due to our underdamped junctions: the inertia causes the junctions to continue to rotate when the applied current is lowered from above its critical value.

It is this hysteresis loop that allows for the existence of breathers in the ladder with dc bias current. In this current range the zero voltage ( $V = 0$ ) and rotating ( $V = V_g$ ) solutions coexist. Then, a discrete breather in the ladder corresponds to when one vertical junction is rotating while the other vertical junctions librate. This solution is easy to conceive in the limit where the vertical junctions are imagined to be completely decoupled. However, whether a localized solution can exist in the ladder will be determined by the strength of the coupling between vertical junctions. This coupling occurs through three mechanisms: fluxoid quantization, self and mutual inductances of the meshes, and the horizontal junctions. Though the effective coupling is a complicated function of the array parameters, it is most strongly controlled by  $h$ . If the anisotropy  $h$  is too large, then the array will not support localized solutions. It has been determined from simulations of the system [8] that  $h = 1/4$  will allow for the existence of breathers in our ladders.

Figure 2 shows some possible solutions for the states of our ladder: (a) the whirling state; (b) the zero-voltage state; (c) a single-site breather solution; and (d) a two-site breather. We have experimentally detected these types of localized solutions [(c) and (d)] by measuring the average dc voltage of the junctions as labeled in (c).

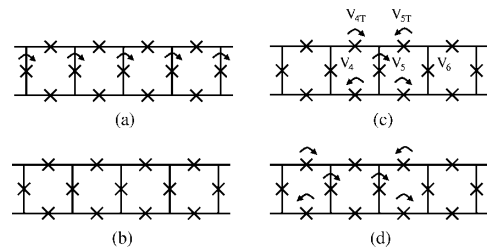


FIG. 2. Schematic of solutions in the array: (a) the whirling state where vertical junctions are rotating, as indicated by the arrows, and horizontal ones librate; (b) the zero-voltage state where there are no rotating junctions; (c) a breather solution where the fifth vertical junction and the nearest horizontal neighbors rotate and the other vertical and horizontal junctions librate; (d) a multisite breather solution where two vertical junctions rotate. Direction of arrows indicates measured voltage polarity.

When we sweep the applied current continuously we find that localized breather solutions can appear spontaneously: they can be thermally excited when the applied current is close to  $I_{dep}$ . However, for our experiments, we have developed a simple reproducible method of exciting a breather: (i) bias the array uniformly to a current below the depinning current; (ii) increase the current injected into the middle vertical junction [labeled  $V_5$  in Fig. 2(c)] until its voltage switches to the gap; (iii) reduce this extra current in the middle junction to zero.

For example, to prepare the initial state in Fig. 3 we started by increasing the applied current to 1.4 mA, which is below  $I_{dep}$ . At this point the array is in the zero-voltage state. We then add an extra bias current to the middle junction (number 5) until it switches to the gap voltage of 2.5 mV, and then we reduce this extra bias to zero. In a sense, we have prepared the initial conditions for the

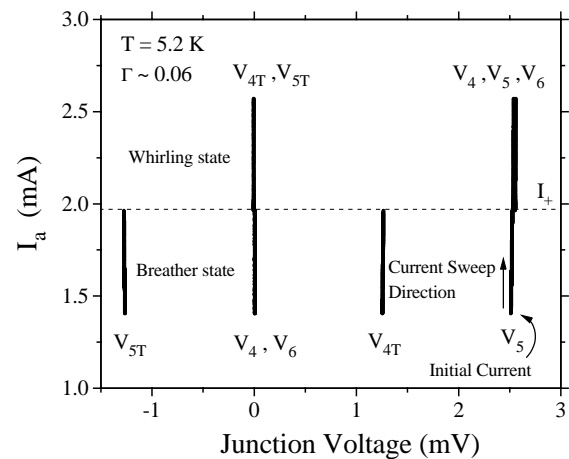


FIG. 3. Measured time-averaged voltages of five junctions in the center of the array as the applied current is increased. We have biased the ladder at 1.4 mA and excited a breather as indicated in the text. Then the applied current is increased. There are two regions in the  $I$ - $V$  plane. Below  $I_r \approx 2$  mA we see the breather; above, the breather becomes unstable and the array switches to the whirling state.

experiment. We can now increase the uniform applied current while simultaneously measuring the voltages of the vertical junctions ( $V_4$ ,  $V_5$ , and  $V_6$ ) and the top two horizontal junctions,  $V_{4T}$  and  $V_{5T}$ , as labeled in Fig. 2(c).

Figure 3 shows the result after we have excited the breather and we have increased the array current. Close to the initial current of 1.4 mA only the fifth vertical junction is at  $V_g$ , and both the fourth and sixth vertical junctions are in the zero-voltage state. This is the breather state shown in Fig. 2(c) and in essence the signature of the localized breather: a vertical junction is rotating while its neighboring vertical junctions do not rotate. We also see that both neighboring horizontal junctions have a voltage magnitude that is precisely half of this value ( $V_{4T} = -V_{5T} = V_5/2$  and  $V_4 = V_6 = 0$ ). Both the magnitude and the sign can be understood by applying Kirchoff's voltage law to top-bottom voltage-symmetric solutions. As sketched in Fig. 2(c), the voltage of the top horizontal junction is equal to the negative of the bottom one. Since the voltage drops around the loop must be zero, the horizontal voltages must be half that of the active vertical junction voltage. As we increase the current, the breather continues to exist until the applied current approaches  $I_+ \approx 2$  mA. At this point the horizontal junctions switch to a zero-voltage state while all of the vertical junctions switch to  $V_g = 2.5$  mV. The array is now in its whirling state as drawn in Fig. 2(a) where  $V_4 = V_6 = V_5 = V_g$  and  $V_{4T} = V_{5T} = 0$ .

If we excite the breather again but instead of increasing the applied current we decrease it, we measure curves typical of Fig. 4. As explained above, we prepare the array in an initial condition with a breather located in junction 5 at 1.4 mA. We then decrease the applied current slowly. We start with the signature measurement of the breather: junction five is rotating at  $V_g$  while  $V_4$  and  $V_6 = 0$ . We also see that the horizontal junctions have the expected value of  $V_g/2$ . As the current is decreased the breather persists until the array is biased at 0.8 mA. The fourth vertical junction then switches to the gap voltage, while  $V_{4T}$  switches to a zero voltage state. The resulting array state is sketched in Fig. 2(d) with  $V_4 = V_5 = V_g$  while  $V_{5T} = -V_g/2$  and  $V_{4T} = V_6 = 0$ . The single-site breather has destabilized by creating a two-site breather.

As the applied current is further decreased beyond the single-site breather instability at  $\approx 0.8$  mA, the voltage of the fourth and fifth vertical junctions decreases, but then suddenly jumps back to  $V_g$ . Then the voltage decreases again, and it again jumps back to  $V_g$ . This second shift corresponds to the sixth junction switching from the zero voltage state to the gap voltage. At this current bias, all of the three measured vertical voltages are rotating. There is a further jump of the voltage as the current decreases. Finally, at 0.2 mA all of the vertical junctions return to their zero-voltage state via a retrapping mechanism analogous to that of a single pendulum.

From these experiments and corroborating numerical simulations we conclude that this shifting of the voltage

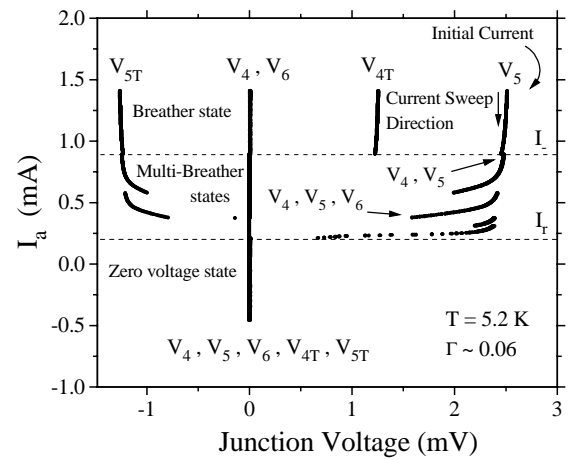


FIG. 4. Measured time-averaged voltages of five junctions in the center of the array as the applied current is decreased. We have biased the ladder at 1.4 mA and excited a breather as indicated in the text. Then the applied current is decreased. There are three regions in the  $I$ - $V$ . The breather state becomes unstable at around  $I_- \approx 0.8$  mA leading to a sequence of shifts at the gap voltage that are interpreted as multisite breather states. The array reaches its zero-voltage state at about  $I_r \approx 0.2$  mA.

back to  $V_g$  corresponds to at least one vertical junction switching from the zero-voltage state to the rotating state. The shapes of the  $I$ - $V$  curves in this multisite breather regime are influenced by the junction nonlinear resistance and the redistribution of current when each vertical junction switches. This redistribution may also govern the evolution of the system after each transition to one of the other possible breather attractors in the phase space of the array. However, the exact nature of the selection process is not yet understood.

The above data were taken at a temperature of 5.2 K. We found four current values of importance: the current when the array returns to the zero voltage,  $I_r$ ; the maximum zero-voltage state current,  $I_{dep}$ ; and the maximum and minimum current for the single-site breather state,  $I_+$  and  $I_-$ . By sweeping the temperature we can study how the current range in which our breather exists is affected by a change of the array parameters.

Figure 5 shows the results of plotting the four special current values versus the damping  $\Gamma$ . To calculate how the junction parameters vary with temperature we take  $I_{cv}(0)R_n = 1.9$  mV and assume that the critical current follows the standard dependence [15]. We estimate  $\Gamma$  from  $I_r$  by the relation  $I_r/N I_{cv} = (4/\pi)\Gamma$  [14], where  $N$  is the number of vertical junctions. The other relevant parameter is the penetration depth,  $\lambda_\perp = \Phi_0/2\pi L_s I_{cv}$ , which measures the inductive coupling in the array. The loop inductance  $L_s$  is estimated from numerical modeling of the circuit. By changing the temperature of the sample, we vary the  $I_{cv}$  of the junction and hence change  $\Gamma$  and  $\lambda_\perp$ . In this sample, the junction parameters can range from  $0.031 < \Gamma < 0.61$  and  $0.04 < \lambda_\perp < 0.43$  as the temperature varies from 4.2 to 9.2 K. In Fig. 5,  $\Gamma < 0.2$

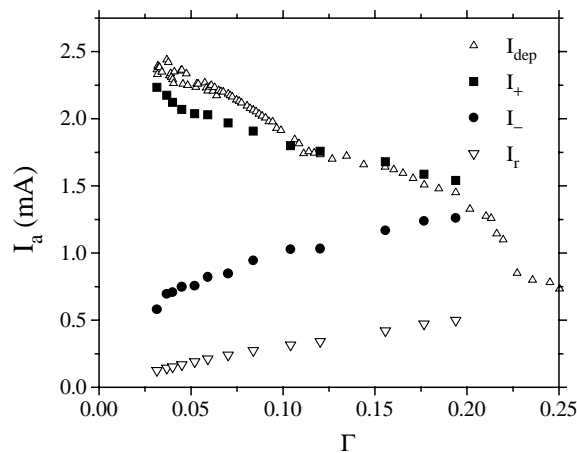


FIG. 5. Existence region of the breather in the current- $\Gamma$  plane.  $\Gamma$  was varied by changing temperature.

corresponds to  $T < 6.7$  K and  $\lambda_{\perp} < 0.05$ . At these low temperatures, there is a larger variation in  $\Gamma$  because of the sensitive dependence of this parameter to the junction's resistance below the gap voltage.

As Fig. 5 shows, the maximum current supported by the breather  $I_+$  is almost equal to  $I_{\text{dep}}$ . We have modeled the rotating junctions as resistors and the nonrotating junctions as shorts. As the driving current is increased, the nearest nonrotating vertical junctions will reach its critical current and begin to rotate, causing the breather to disappear. In the simplest case, when we ignore any circulating Meissner currents, this model yields  $I_+/NI_{cv} = (2h + 2)/(3h + 2) = 0.9$ . Since  $I_{\text{dep}}$  is roughly  $NI_{cv}$ , the depinning current is the upper bound for the applied current that the breather can support.

We suggest two possible instability mechanisms that can determine  $I_-$ . One possibility is via a retrapping mechanism similar to that of a single junction. For this single site breather, the middle vertical junction and the neighboring horizontal junctions rotate. As the current is decreased, a point is reached where the current drive is not sufficient to support the rotations and the breather destabilizes. This physical picture gives  $I_-/NI_{cv} = (2h + 2)(4/\pi)\Gamma$ . So that for our parameters,  $I_-$  should be 2.5 times larger than  $I_r$ , as it is approximately in Fig. 5. A second possible instability can occur when the breather loses energy by exciting lattice eigenmodes. In our experiments, the breather always loses stability at voltages close to  $V_g$ . For our parameter range,  $V_g$  is larger than the voltages for the lattice eigenmodes, thus our data seem to favor a retrapping mechanism. Last, we add that since  $I_{\text{dep}}$  and consequently  $I_+$  decrease with  $\Gamma$ , there also seems to be a critical damping where the breather will cease to exist. Experimentally we did not find a breather for  $\Gamma > 0.2$ .

By varying the external current and temperature we have studied the domain of existence of these localized solutions. The study leads to some interesting theoretical questions on how the current values shown in Fig. 5 depend on parameter values or how to unfold the dynamics when  $I_+$  coincides  $I_-$ . These questions are under current study. In addition we have also found, but not discussed here, breathers which are not top-bottom voltage symmetric [8], in which only the top (bottom) horizontal junctions rotate while the bottom (top) junctions are in the zero-voltage state.

We thank S. H. Strogatz, A. E. Duwel, F. Falo, L. M. Floría, and P. J. Martínez for insightful discussions. J. J. M. thanks the Fulbright Commission and the MEC (Spain) for financial support. This work was supported by NSF Grant No. DMR-9610042 and DGES (PB95-0797 and PB98-1592).

*Note added.*—After the submission of this paper we learned of a similar experimental work [16] which reports the observation of multisite breathers in Josephson-junction ladders.

- 
- [1] R. S. MacKay and S. Aubry, *Nonlinearity* **7**, 1623 (1994).
  - [2] J.-A. Sepulchre and R. S. MacKay, *Nonlinearity* **10**, 679 (1997).
  - [3] S. Aubry, *Physica (Amsterdam)* **103D**, 201 (1997).
  - [4] S. Flach and C. R. Willis, *Phys. Rep.* **295**, 181 (1998).
  - [5] R. Lai and A. J. Sievers, *Phys. Rev. Lett.* **81**, 1937 (1998).
  - [6] M. Peyrard, *Europhys. Lett.* **44**, 271 (1998).
  - [7] L. M. Floría, J. L. Marín, P. J. Martínez, F. Falo, and S. Aubry, *Europhys. Lett.* **36**, 539 (1996).
  - [8] J. J. Mazo, E. Trías, and T. P. Orlando, *Phys. Rev. B* **59**, 13 604 (1999).
  - [9] S. Flach and M. Spicci, *J. Phys. Condens. Matter* **11**, 321 (1999).
  - [10] J. Aubrecht, A. F. Vakakis, T.-C. Tsao, and J. Bentsman, *J. Sound Vib.* **195**, 629 (1996).
  - [11] A. F. Vakakis, A. N. Kounadis, and I. G. Raftoyiannis, *Earthq. Eng. Struct. Dyn.* **28**, 21 (1999).
  - [12] B. I. Swanson *et al.*, *Phys. Rev. Lett.* **82**, 3288 (1999).
  - [13] U. T. Schwarz, L. Q. English, and A. J. Sievers, *Phys. Rev. Lett.* **83**, 223 (1999).
  - [14] K. K. Likharev, *Dynamics of Josephson Junctions and Circuits* (Gordon and Breach, New York, 1986).
  - [15] V. Ambegaokar and A. Baratoff, *Phys. Rev. Lett.* **10**, 486 (1963).
  - [16] P. Binder *et al.*, following Letter, *Phys. Rev. Lett.* **84**, 745 (2000).